A class of memristive Hénon maps

Zhihao Wang[1] , Chunbiao Li[1 a)], Yongxin Li[1], Irene Moroz[2], Haiyan Fu[3]

[1]*School of Artificial Intelligence, Nanjing University of Information Science & Technology, Nanjing 210044, China*
[2]*Mathematical Institute, University of Oxford, Oxford OX26GG, UK*
[3]*Collaborative Innovation Center of Memristive Computing Application (CICMCA), Qilu Institute of Technology, Jinan, China*

ABSTRACT

Memristor, the electronic component, is introduced in the Hénon map and is studied extensively. Several chaotic maps are proposed by constructing the memristors through nonlinear functions such as absolute value functions, trigonometric functions, and activation functions. It is found that in a part of the proposed chaotic maps, the local offset boosting of the system variable can be guided by a single parameter. Not only that, the generation of homogeneous multistability can be controlled by the initial conditions of the systems. Moreover, the number of homogeneous attractors produced changes when the system parameters are varied. In addition, the control of chaos can be achieved by adjusting the excitation frequency of the memristor. The theoretical results and numerical laws presented in this paper are verified by circuit implementation based on the microcontroller unit.

1. Introduction

Chaotic signal [1–3] is a type of signal that exhibits irregularity, aperiodicity, and high complexity over time. The primary characteristics of chaotic signals are broad frequency spectrum, randomness, and determinism. The generation of chaotic signals typically involves nonlinear dynamical systems [4], such as the Lorenz system and the Logistic map. These systems possess the property of sensitive dependence on initial conditions, wherein small changes in initial conditions can lead to significant differences in the systems' evolution. Due to these characteristics, chaotic signals have attracted extensive research interest in various fields, including communication [5], cryptography [6], and biology [7]. In the field of chaotic system research, the control of chaotic signals has always been a popular topic of investigation [8]. To steer the behaviors of chaotic systems towards desired states or achieve specific functionalities, researchers have explored various control strategies, including offset boosting [9,10], the existence of multistability [11], and the introduction of memristors [12–14].

Chaotic systems are characterized by the sensitivity to initial conditions, the complexity, and unpredictable behavior, which makes it great challenging to control such systems.

a) Corresponding author. E-mail address: goontry@126.com; chunbiaolee@nuist.edu.cn

Offset boosting provides a simple yet effective means for controlling the system's trajectory [15]. Offset boosting is a common control method for chaotic signals even a discrete map [16], which involves introducing a constant offset signal to alter the dynamic behaviors of the system. This external parameter serves as a control unit that can shift the system's orbit in a desired direction. This method allows for the adjustment of the attractor positions in chaotic systems, enabling control and regulation of the systems [17,18]. By adjusting the magnitude and temporal variations of the offset boosting parameter, a transition can be achieved from periodic to chaotic motion. Offset boosting can modify the stability, and periodicity, or generate new attractors in the systems [19,20]. It has an impact on the multistability and coexistence of attractors in chaotic systems [21,22]. Multistability is an important phenomenon in chaotic systems, indicating the simultaneous existence of multiple stable attractors. By changing the initial conditions of the systems [23], homogeneous or heterogeneous attractors can be generated. The presence of multistability provides chaotic systems with increased degrees of freedom and richer dynamic behaviors, offering broader potential applications in information processing and random number generation [24,25]. Through the design of appropriate control strategies, it is possible to achieve transitions from one stable state to another, thereby controlling and regulating chaotic systems [26]. In addition to offset boosting and multistability, the introduction of memristors also has a significant impact on the control and dynamic behaviors of chaotic systems [27]. A memristor is an electronic component with memory effects, where its resistance varies with voltage or current and retains the memory for a certain period of time [28]. Incorporating memristors into chaotic systems can alter their dynamic characteristics and introduce adaptive capabilities [29]. The introduction of memristors extends the state space of chaotic systems, enhances their nonlinear properties, and introduces more complex behaviors and a wider range of control strategies [30].

Many important results have been achieved in the study of continuous chaotic systems [26, 27]. Researchers have revealed the basic principles, dynamical behaviors, and control methods of chaotic systems through mathematical modeling, simulation experiments, and real circuit implementation [33]. Continuous chaotic systems find wide applications in areas such as communication encryption, random number generation, chaotic modulation, and chaos synchronization [34,35]. However, there are certain gaps in the study of discrete chaotic signals. The study of discrete chaotic systems is relatively limited, especially in the drilling of offset boosting, multistability, and memristors. This limitation restricts the development of discrete systems in information processing and control applications. Therefore, to address this gap, we have constructed a class of memristive Hénon maps intending to explore the dynamic behaviors and potential applications of discrete chaotic signals. The proposed systems take into account factors such as offset boosting, multistability, and memristors, and further investigate their effects in the field of the control of chaos.

The main contributions of this work are as follows:
(1) Based on the Hénon map, we successfully introduce the memristor as an electronic

component in the proposed systems. By employing various nonlinear functions, several novel discrete chaotic maps are constructed. These nonlinear functions include absolute value functions, trigonometric functions, and activation functions widely used in neural networks to enhance the nonlinear properties of the systems and enrich their dynamic behaviors.
(2) In a part of the proposed chaotic systems, the one-dimensional offset boosting of the systems is achieved through a parameter, allowing for the adjustment of the systems' dynamic behaviors. This parameter can be regarded as an one-dimensional offset boosting of the systems. By tuning its magnitude and variation, the extent of deviation and trajectories of the attractors can be altered.
(3) In the proposed systems, the coexistence of homogeneous attractors is discovered when the initial values of the systems undergo periodic variations. The generation of these attractors is induced by slight changes in the system parameters. By fine-tuning these parameters, researchers can control the generation of different attractors and achieve regulation and control of the systems' states.
(4) By adjusting the external excitation frequency of the memristors, the influence on the systems' dynamic behaviors is achieved. When the excitation frequency is in a suitable range, the nonlinear feedback of the memristors can be enhanced. The introduction of the excitation frequency enables the control of chaotic systems.
(5) A circuit implementation based on CH32 is employed to validate the proposed systems' offset boosting and the multistability controlled by initial conditions.

The remainder of this paper is summarized below. In Section 2, a class of memristive Hénon map is proposed and the system parameter settings of the proposed maps are shown. In Section 3, the local offset boosting of the system variables is demonstrated. In Section 4, the coexistence of homogeneous attractors generated based on the system's initial conditions is shown. In Section 5, it is shown that adjusting the excitation frequency of the memristors thereby affects the dynamic behaviors of the chaotic systems. In Section 6, the proposed chaotic maps are implemented through a circuit based on the CH32 platform, and the offset boosting and coexistence of homogeneous attractors are demonstrated on its basis. In Section 7, the conclusion of this paper is shown.

2. Memristor- embedded Hénon maps

Inspired by the above-mentioned work, we construct a class of memristive Hénon maps as follows:

$$\begin{cases} x_{n+1} = 1 - ax_n^2 - f\left(y_n\right)x_n \\ y_{n+1} = cy_n + bx_n \end{cases} \tag{1}$$

In Eq. (1), a, b, and c are the three system parameters, and $f(y_n)$ is a nonlinear function about y_n, which contains the absolute value function, trigonometric functions and activation functions. For the classic Hénon map, $f(y_n) = y_n$ and $c = 0$.
According to Eq. (1), six chaotic maps are constructed as shown in Table 1. Six different

expressions and corresponding system parameters are shown in Table 1. It is worth noting that we successfully construct six chaotic maps by using different nonlinear functions to act as different memristors. In addition, the Lyapunov exponents (LEs) and Kaplan-Yorke fractal dimension (D_{KY}) corresponding to these maps are available in Table 1. Lyapunov exponents are used to measure the sensitive dependence and chaotic behaviors of dynamical systems. The Wolf algorithm is here employed to get Lyapunov exponents. Both $x(n)$ and $y(n)$ are initially set to 0. The system variables $x(n+1)$ and $y(n+1)$ are taken into consideration after 10,000 iterations. Kaplan-Yorke fractal dimension is a measure of bifurcation and chaotic behaviors in dynamical systems. Kaplan-Yorke fractal dimension gives the attractor dimension as an upper bound and is calculated as follows:

$$D_{KY} = j + \frac{1}{\left|LE_{j+1}\right|}\sum_{i=1}^{j} LE_i \tag{2}$$

where j is the maximum value that makes $\sum_i^j LE_i \geq 0$.

Table 1
Six chaotic maps with $(x_0, y_0) = (0, 0)$.

Models	Equations	Parameters	LEs	D_{KY}
MHM1	$\begin{cases} x_{n+1} = 1 - ax_n^2 - \left(0.77 + 1.1\left\|y_n\right\|\right)x_n \\ y_{n+1} = cy_n + bx_n \end{cases}$	$a = 0.7$ $b = 0.2$ $c = 1$	0.1188, -0.1609	1.74
MHM2	$\begin{cases} x_{n+1} = 1 - ax_n^2 - \left(1.26 + \tanh\left(y_n\right)\right)x_n \\ y_{n+1} = cy_n + bx_n \end{cases}$	$a = 0.1$ $b = 1$ $c = 1$	0.0577, -0.0894	1.65
MHM3	$\begin{cases} x_{n+1} = 1 - ax_n^2 - 1.8\cos\left(y_n\right)x_n \\ y_{n+1} = cy_n + bx_n \end{cases}$	$a = 0.01$ $b = 0.1$ $c = 1$	0.2514, -0.0031	2
MHM4	$\begin{cases} x_{n+1} = 1 - ax_n^2 - 1.9\sin\left(y_n\right)x_n \\ y_{n+1} = cy_n + bx_n \end{cases}$	$a = 0.03$ $b = 0.08$ $c = 1$	0.2791, -0.1543	2
MHM5	$\begin{cases} x_{n+1} = 1 - ax_n^2 + 1.5\cos\left(y_n\right)x_n \\ y_{n+1} = cy_n + bx_n \end{cases}$	$a = 1$ $b = 1$ $c = -1$	0.2110, 0.0123	2
MHM6	$\begin{cases} x_{n+1} = 1 - ax_n^2 - 2\sin\left(y_n\right)x_n \\ y_{n+1} = cy_n + bx_n \end{cases}$	$a = 1$ $b = 0.1$ $c = -1$	0.07, 0.0083	2

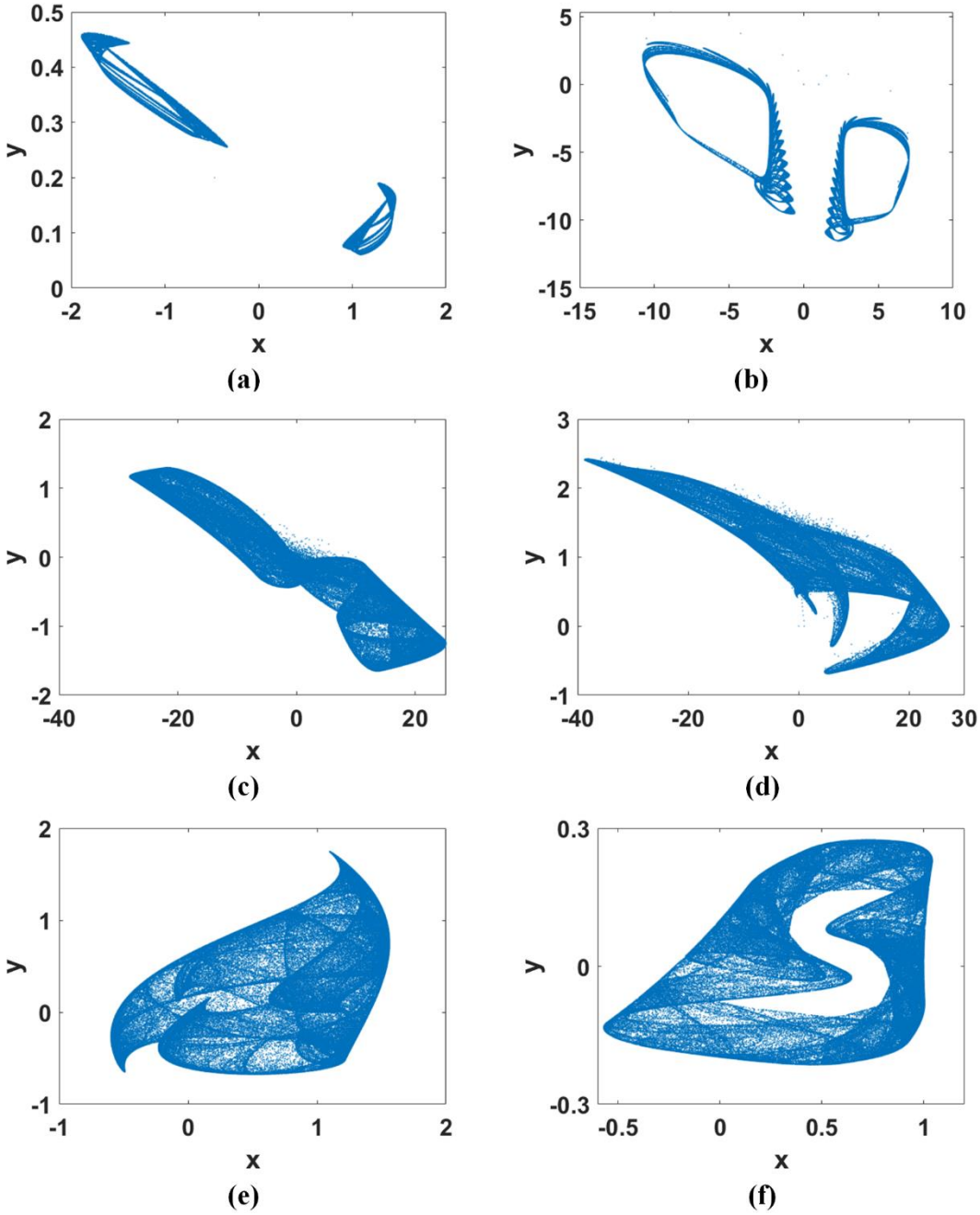

Fig. 1. Attractors of the models with $(x_0, y_0) = (0, 0)$: (a) MHM1, (b) MHM2, (c) MHM3, (d) MHM4, (e) MHM5, (f) MHM6.

In order to have a visual observation of the attractors generated by these systems, Fig. 1 illustrates the dynamical behaviors of these six attractors. Fig. 1 shows the phase trajectories of the six chaotic maps at the initial value $(x_0, y_0) = (0, 0)$ and for different system parameter settings. In Fig. 1, different memristors modulate the dynamical behaviors of the attractors and increase the nonlinear properties of the systems. The introduction of the memristors extends the state space of the chaotic system. Please note, the sequences and phase orbits are derived by 100,000 iterations, with the ignorance of first 5,000 iterations to remove the transient.

In addition to constructing chaotic systems using the common functions mentioned above, we also try to use many interesting functions for constructing chaotic systems. ReLU function, Sigmoid function and Softsign function are included, which are frequently used as activation functions in neural networks. Table 2 shows in detail these chaotic systems where activation functions are successfully introduced. In Table 2, the equations, parameters, Lyapunov exponents and Kaplan-Yorke fractal dimension of these systems are shown in detail.

In Fig. 2, the phase trajectories of these chaotic maps are shown. We are surprised to find that these maps, constructed by the activation functions, produce attractors that are very similar in shape. In particular, the attractor produced by MHM7 constructed by the ReLU function is identical to the attractor of MHM1 constructed by the absolute value function in both shape and value domain. This is due to the fact that at these parameter values, the values of the $y(n)$ sequences in both systems are greater than or equal to 0, and the ReLu function and the absolute value function act on the $y(n)$ sequences in the same way. Therefore, they exhibit the same dynamic behaviors under the effect of the same parameters, as shown in Fig. 3(a). In addition to this, MHM8 constructed by the Sigmoid function and MHM9 constructed by the Softsign function exhibit similar phase trajectories under similar system parameters. This is because the two activation functions as shown in Fig. 3(b) are very close to each other in the $y(n)$ range under the system parameters.

Table 2 Chaotic maps with activation functions

Models	Equations	Parameters	LEs	D_{KY}
MHM7	$\begin{cases} x_{n+1} = 1 - ax_n^2 - \left(0.77 + 1.1\mathrm{ReLU}\left(y_n\right)\right)x_n \\ y_{n+1} = cy_n + bx_n \end{cases}$	$a = 0.7$ $b = 0.2$ $c = 1$	0.1188, -0.1609	1.74
MHM8	$\begin{cases} x_{n+1} = 1 - ax_n^2 - \left(0.81 + 0.3\mathrm{Sigmoid}\left(y_n\right)\right)x_n \\ y_{n+1} = cy_n + bx_n \end{cases}$	$a = 0.58$ $b = 5$ $c = 1$	0.1379, -0.1215	2
MHM9	$\begin{cases} x_{n+1} = 1 - ax_n^2 - \left(0.825 + 0.33\mathrm{Softsign}\left(y_n\right)\right)x_n \\ y_{n+1} = cy_n + bx_n \end{cases}$	$a = 0.58$ $b = 5$ $c = 1$	0.1721, -0.2263	1.76

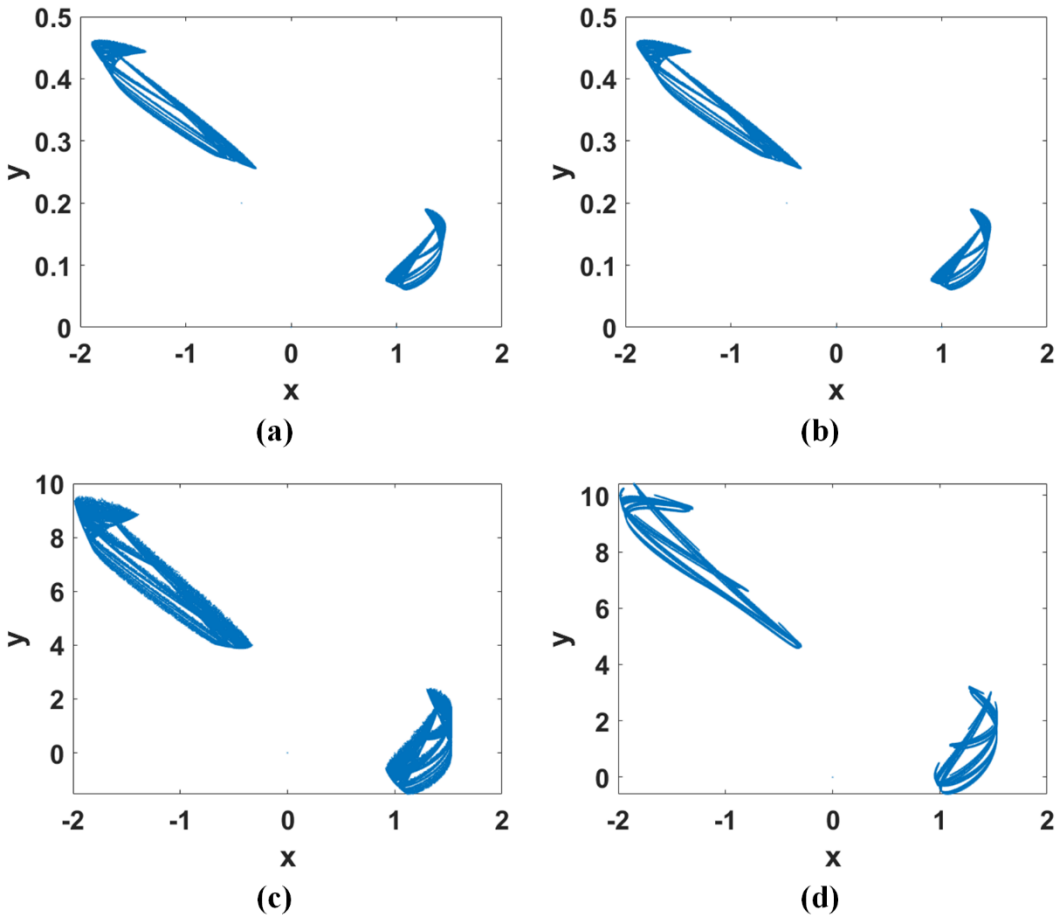

Fig. 2. Similar attractors generated by chaotic maps constructed with different functions: (a) MHM1, (b) MHM7, (c) MHM8, (d) MHM9.

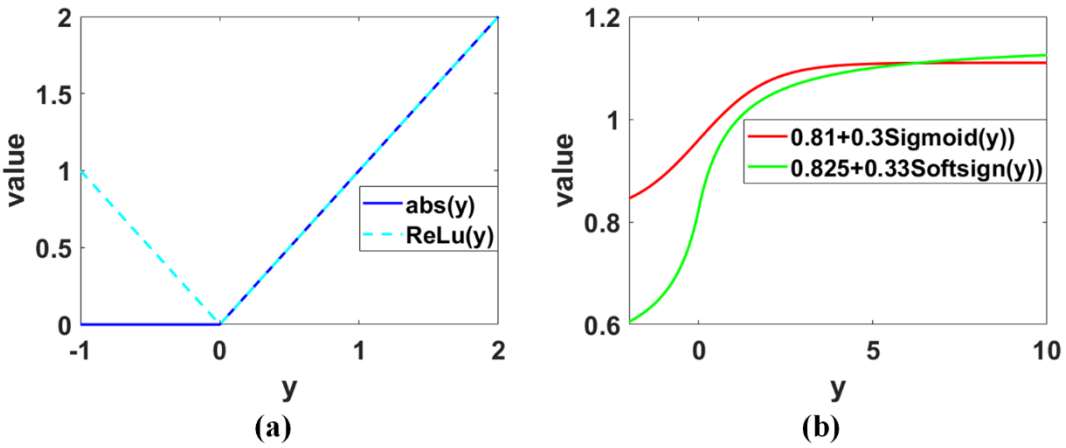

Fig. 3. Functions used to construct chaotic systems: (a) when the variable y is greater than or equal to 0, the absolute value function and the ReLU function have the same effects on y, (b) Sigmoid function and Softsign function exhibit similar properties under the system parameters.

3. Offset boosting relying on a single parameter

Offset boosting of chaotic systems is a method of changing the behavior of a chaotic system by introducing external signals or control parameters. This method is often used to control and adjust the properties of chaotic systems or to generate specific chaotic sequences. In discrete systems, there are usually two ways to implement offset boosting. The first method is to introduce external parameters into the current system to control the offset boosting of the discrete sequences. The second method is to change the initial conditions of the system and thus achieve offset boosting. In the chaotic maps proposed in this paper, models MHM1, MHM2, MHM3, MHM4, MHM7, MHM8 and MHM9 can be locally offset boosted by the first method. For example, in MHM1, when the variable y obtains an offset boosting d_1, the model MHM1 should be modified as follows:

$$\begin{cases} x_{n+1} = 1 - ax_n^2 - \left(0.77 + 1.1\left|y_n + d_1\right|\right)x_n \\ y_{n+1} = c\left(y_n + d_1\right) + bx_n - d_1 \end{cases} \tag{3}$$

Since the system parameter $c = 1$ in MHM1, the offset boosting parameter d_1 of the second expression in Eq. (3) can be removed. This means that only one parameter d_1 is enough to achieve the offset boosting of the variable y, as shown in Eq. (4).

$$\begin{cases} x_{n+1} = 1 - ax_n^2 - \left(0.77 + 1.1\left|y_n + d_1\right|\right)x_n \\ y_{n+1} = y_n + bx_n \end{cases} \tag{4}$$

In order to better demonstrate the effect of the parameter d_1 on the offset boosting of the variable y, Fig. 4 shows the dynamic behaviors of MHM1 under different settings of the parameter d_1. Fig. 4(a) and (b) show the offset boosting of the parameter d_1 to the phase trajectories and waveform of the map (4) with different parameter settings, respectively. As shown in Fig. 4(c) and (d), the bifurcation diagram and invariant Lyapunov exponents indicate that the parameter d_1 achieves offset boosting without changing the system dynamics.

In the chaotic map proposed in this paper, the offset boosting of system variable y can be achieved when the system parameter $c = 1$. Therefore, there also exists the offset boosting parameter d_2 in the model MHM2. The offset boosting of the variable y in MHM2 can be achieved by a single parameter d_2, as shown in Eq. (5):

$$\begin{cases} x_{n+1} = 1 - 0.1x_n^2 - \left(1.26 + 0.3\tanh\left(y_n + d_2\right)\right)x_n \\ y_{n+1} = y_n + x_n \end{cases} \tag{5}$$

Fig. 5 illustrates the dynamic behaviors of MHM2 with different settings of the offset boosting parameter d_2. Fig. 5(a) and (b) demonstrate the offset boosting of the phase trajectories and waveform of the map (5) with different settings of the parameter d_2, respectively. As shown in Fig. 5(c) and (d), the bifurcation diagram and invariant Lyapunov exponents indicate that the parameter d_2 achieves offset boosting without changing the system dynamics. Fig. 6(a) and (b) demonstrate the average value of the variable y in MHM1 and MHM2, as the offset boosting parameters are changed,

respectively.

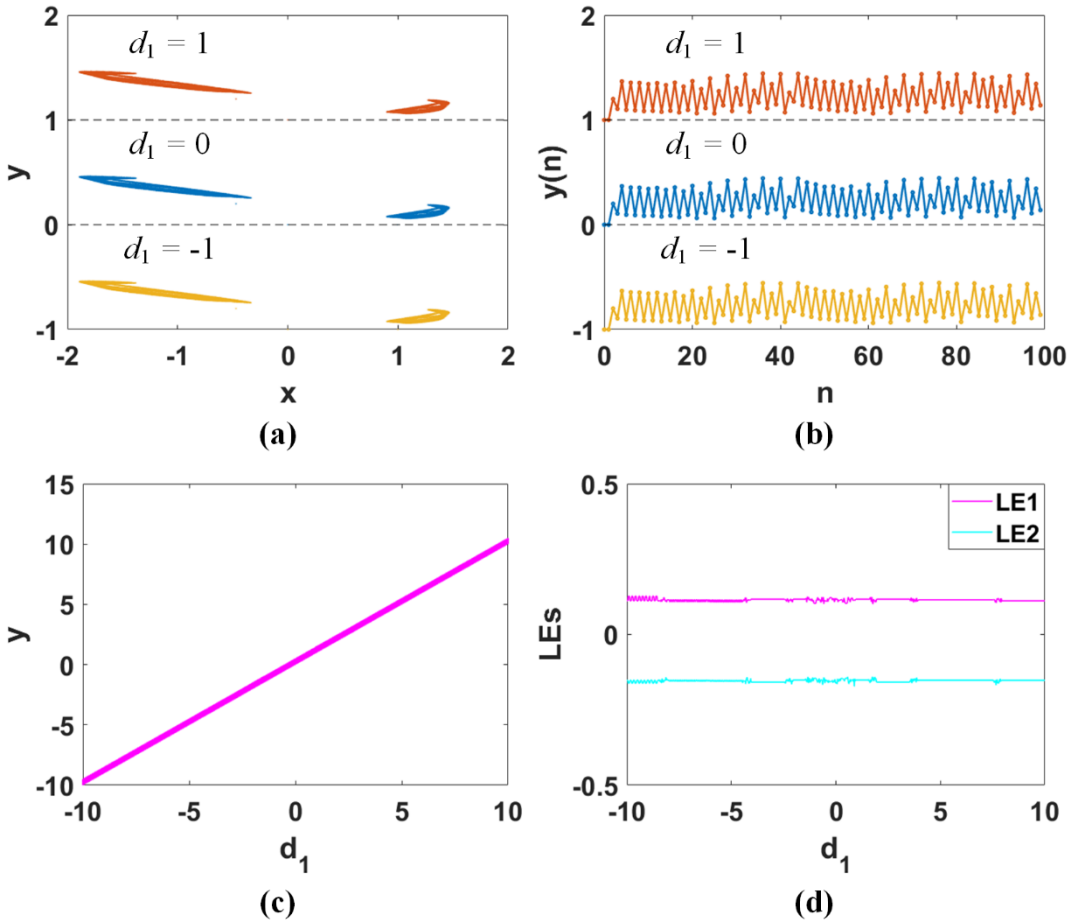

Fig. 4. Offset boosting of MHM1: (a) parameter d_1 changes the offset boosting of the phase orbits, where blue: $d_1 = 0$, red-orange: $d_1 = 1$, gold: $d_1 = -1$, (b) the offset boosting of waveform $y(n)$ is adjusted by parameter d_1, where blue: $d_1 = 0$, red-orange: $d_1 = 1$, gold: $d_1 = -1$, (c) bifurcation diagram, (d) Lyapunov exponents.

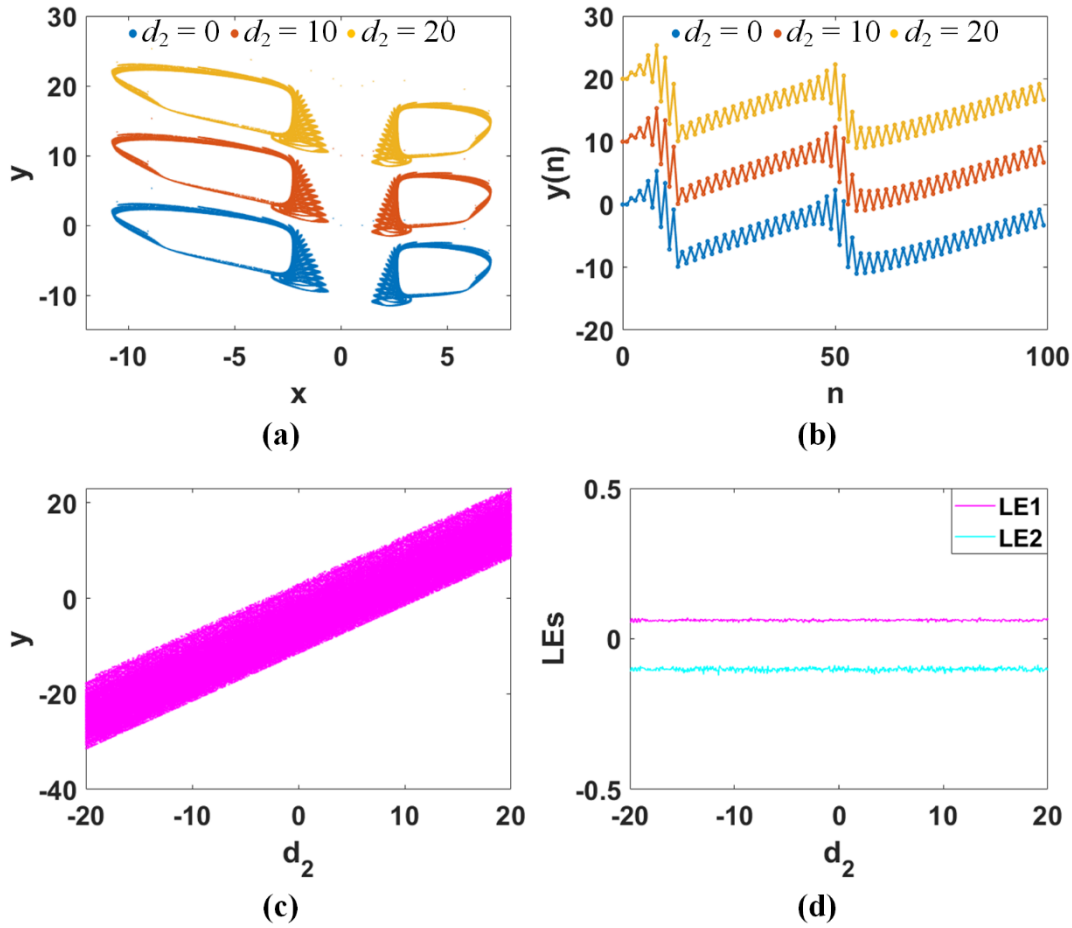

Fig. 5. Offset boosting of MHM5: (a) parameter d_2 changes the offset boosting of the phase orbits, where blue: d_2 = 0, red-orange: d_2 = 10, gold: d_2 = 20, (b) the offset boosting of waveform $y(n)$ is adjusted by parameter d_2, where blue: d_2 = 0, red-orange: d_2 = 10, gold: d_2 = 20, (c) bifurcation diagram, (d) Lyapunov exponents.

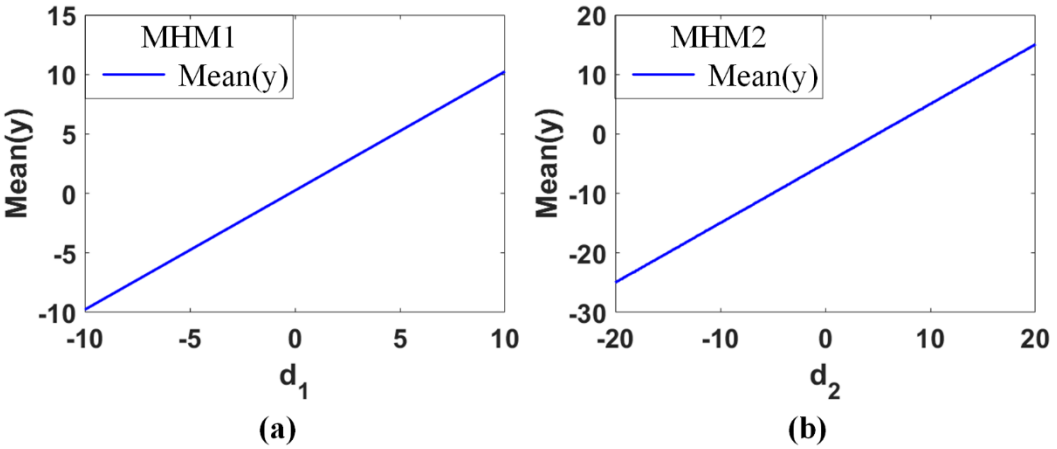

Fig. 6. The mean value of $y(n)$ varies with the offset boosting parameter: (a) average value of variable y of MHM1, (b) average value of variable y of MHM2.

4. Offset-oriented multistability

Multistability is an important phenomenon in chaotic systems. It indicates the existence of multiple fixed points or attractors in the systems. These attractors correspond to different system parameters or initial conditions. In continuous systems, symbolic functions or trigonometric functions are usually utilized to construct chaotic systems with multistability. Inspired by this, we introduce trigonometric functions to construct discrete chaotic systems with multistability properties, i.e., MHM3, MHM4, MHM5, and MHM6 in Table 1. In these systems, we construct discrete systems with coexisting homogeneous attractors by introducing two kinds of periodic functions, namely, the sine function and the cosine function. By changing the initial value of $y(0)$, these systems can successfully access the homogeneous attractors.

As shown in Fig. 7, the coexisting homogeneous attractors produced by MHM3 and MHM4 are controlled by the initial conditions. When $y(0)$ gets periodic feedback, both systems generate a single homogeneous attractor. Fig. 7(a) shows the system MHM3 generates homogeneous attractors when $y(0)$ is taken as $\pm 2\pi$ and $\pm 4\pi$, respectively. Fig. 7(b) demonstrates the system MHM4 generates homogeneous attractors when $y(0)$ is taken as $\pm 2\pi$ and $\pm 4\pi$, respectively. Fig. 8 and Fig. 9 show the dynamic analysis of MHM3 and MHM4, respectively, including the bifurcation diagrams and Lyapunov exponents under different initial conditions.

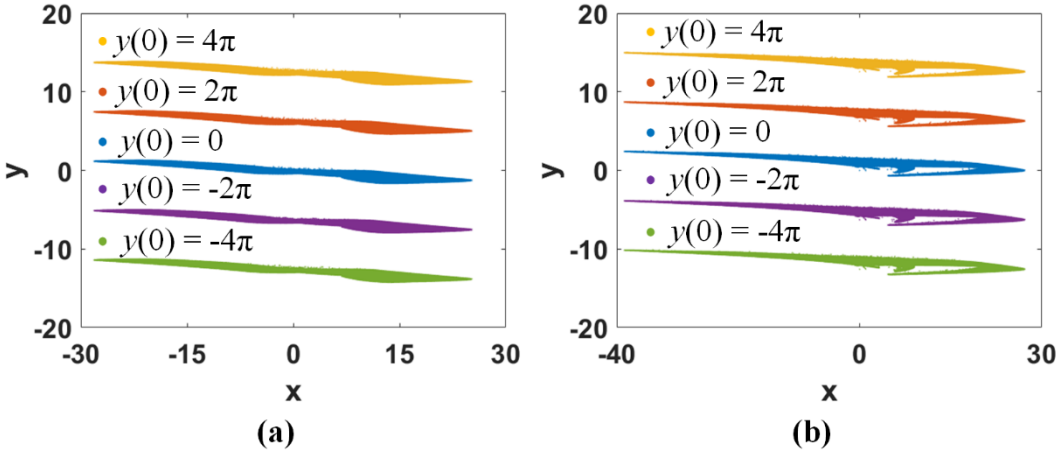

Fig. 7. Coexisting attractors with different offset levels: (a) MHM3, (b) MHM4.

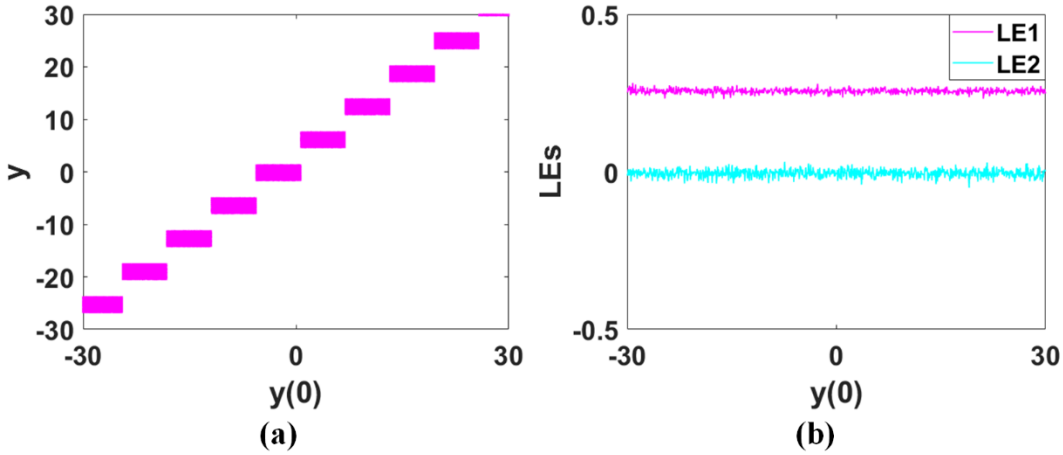

Fig. 8. Dynamics analysis of MHM3: (a) bifurcation diagram, (b) Lyapunov exponents.

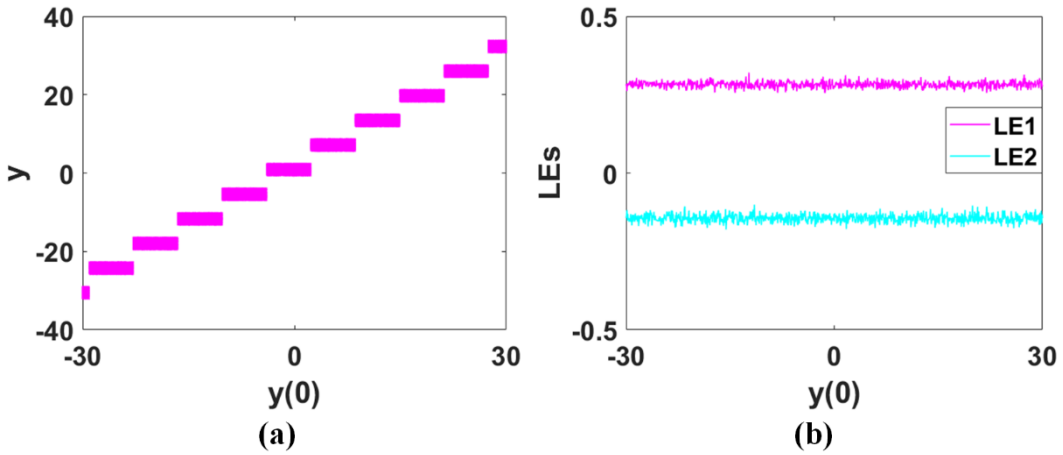

Fig. 9. Dynamics analysis of MHM4: (a) bifurcation diagram, (b) Lyapunov exponents.

Moreover, the multistability phenomenon also exists for the maps MHM5 and MHM6 when the system parameter c = -1. Unlike the homogeneous multistability phenomenon described above, two homogeneous attractors are generated at a time when the initial value of $y(0)$ of MHM5 or MHM6 receives periodic feedback. That is to say, MHM5 or MHM6 produces twice as many attractors as MHM3 or MHM4. As shown in Fig. 10, the systems produce two homogeneous attractors when the initial values of $y(0)$ are 2π and 4π, respectively. In this case, the phenomenon of coexisting homogeneous multistability appears. Fig. 11 and Fig. 12 show the dynamics analysis of the systems MHM5 and MHM6, respectively, including the bifurcation diagrams and Lyapunov exponents under different initial conditions.

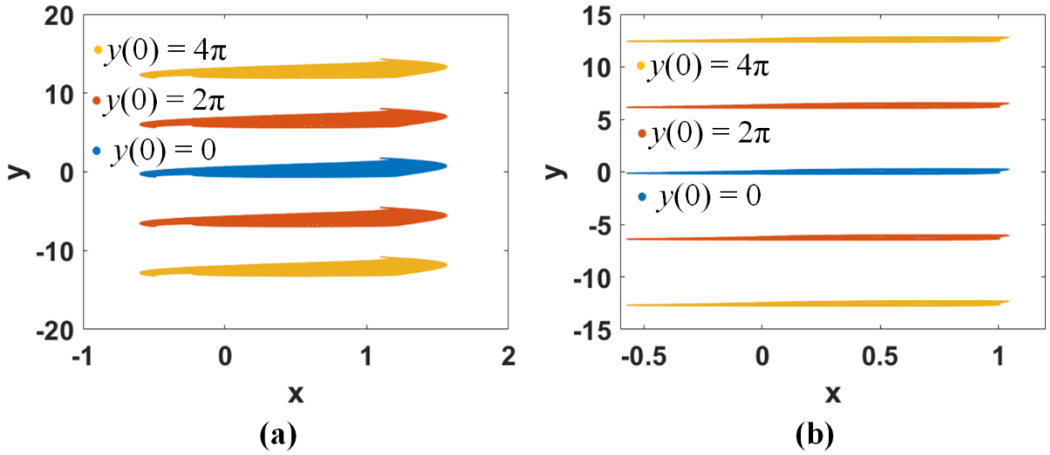

Fig. 10. Generation of attractors with different initial values of $y(0)$: (a) phase trajectories with different initial values of $y(0)$ of MHM5, (b) phase trajectories with different initial values of $y(0)$ of MHM6.

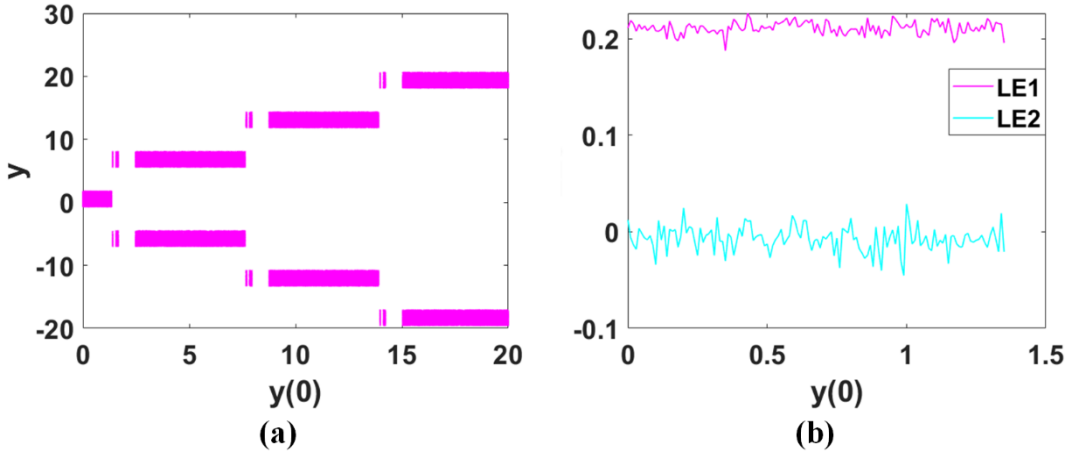

Fig. 11. Dynamics analysis of MHM5: (a) bifurcation diagram, (b) Lyapunov exponents.

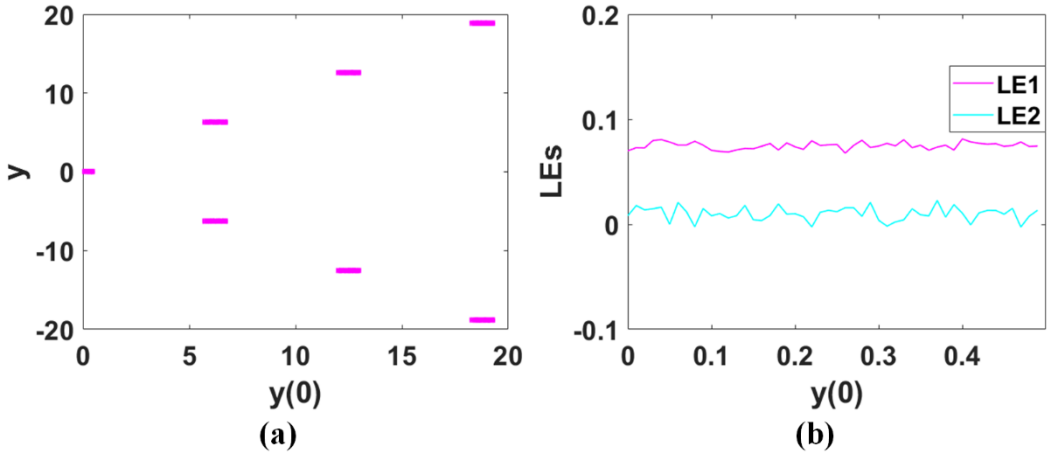

Fig. 12. Dynamics analysis of MHM6: (a) bifurcation diagram, (b) Lyapunov exponents.

5. Excitation frequency of the memristor

By adjusting the excitation frequency of the memristor, the response state of the memristor can be adjusted, which further controls the systems' dynamical behaviors. This tuning allows the system to transition among different dynamics, e.g. from periodic to chaotic behaviors. In addition, the adjustment of the frequency of the memristor changes the number and type of coexisting attractors in phase space. This type of control provides a novel means for regulating chaotic sequences.

Take the MHM3 system as an example, introducing the time scale factor s, the following equations are obtained:

$$\begin{cases} x_{n+1} = s\left(1 - ax_n^2 - 1.8\cos\left(y_n\right)x_n - x_n\right) + x_n \\ y_{n+1} = cy_n + bx_n \end{cases} \tag{6}$$

Here the inherent differential constraint relation of the memristor remains unchanged, while only the dynamical speed of the external excitation variable is changed. Fig. 13 illustrates the bifurcation diagram and Lyapunov exponents for the time scale s in the range (0, 1.1). When s is in the range of (0, 0.75), the system is in a divergence state. When s is in the range of (0.75, 0.95), the system is in a period state. Fig. 14 demonstrates the changes in the system's period state caused by the time scale s in different cases. As shown in Fig. 15, the system is in a chaotic state when s is in the range of (0.95, 0.99) and (1, 1.1). Different values of s correspond to different phase trajectories as shown in Fig. 15. The changes in frequency affect not only the shape of the phase trajectories but also the number of attractors generated. By analyzing the phase trajectories in Fig. 15, it can be found that an increase in s within a certain range enhances the nonlinear properties of the system, thus increasing the number of attractors. When s is greater than 1.1, the linear feedback of the memristor is enhanced and the nonlinear feedback is weakened, so the chaotic state cannot be reached.

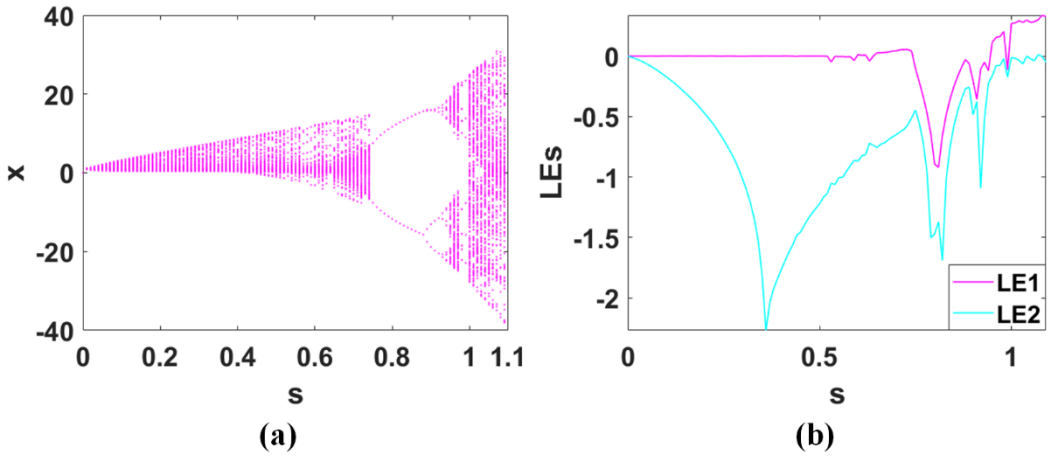

Fig. 13. Dynamic analysis of MHM3: (a) bifurcation diagram, (b) Lyapunov exponents.

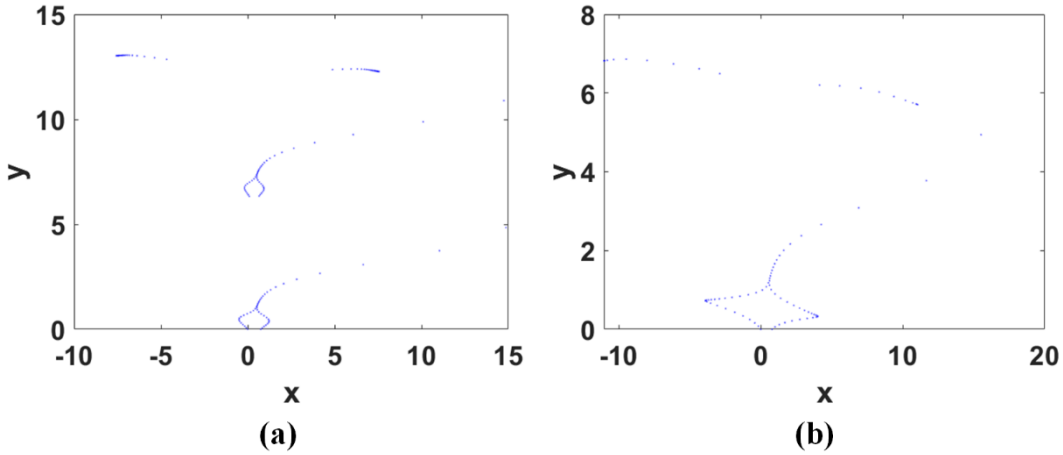

Fig. 14. Period state of MHM3 with different values of s: (a) s = 0.75, (b) s = 0.79.

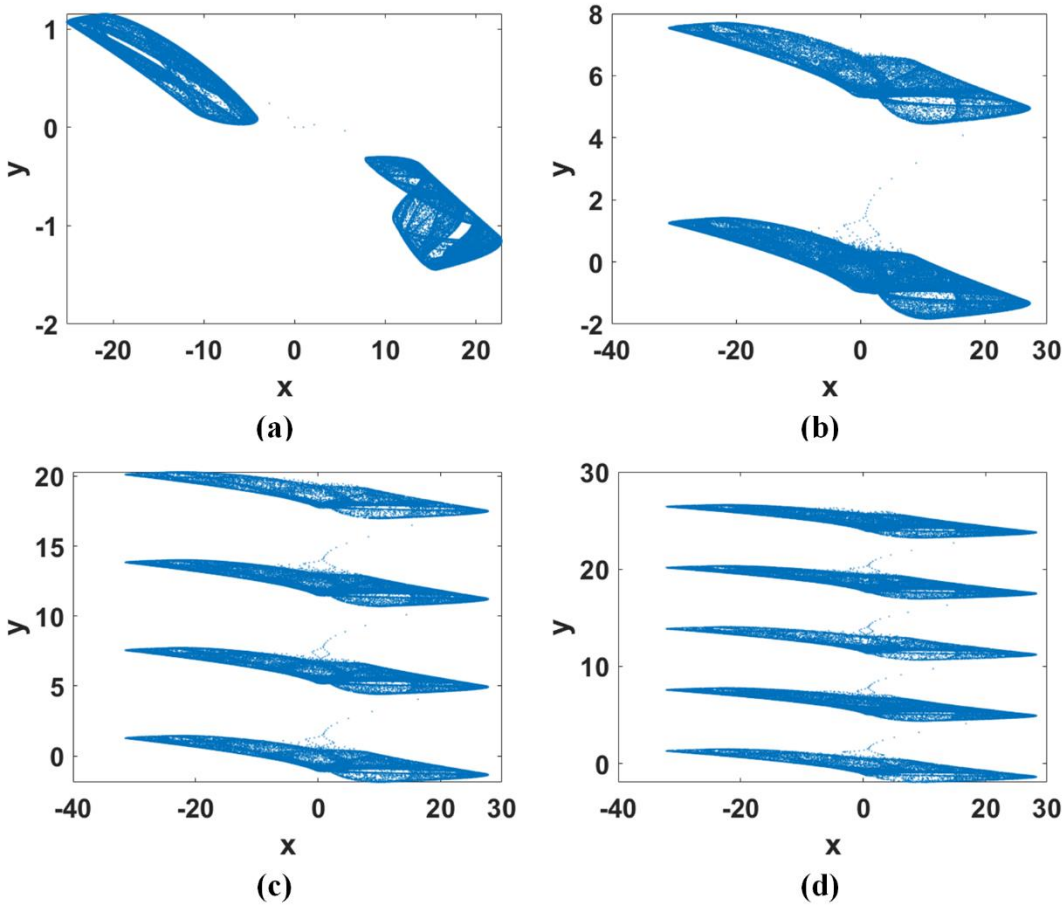

Fig. 15. Different phase trajectories of MHM3 with different settings of s: (a) s = 0.97, (b) s = 1.026, (c) s = 1.032, (d) s = 1.038.

6. Circuit verification based on CH32 platform

The CH32V307 is a 32-bit microcontroller with an embedded RISC-V core and hardware floating-point unit, with a maximum frequency of 144MHz. RISC-V, an open-source instruction set architecture, follows the principles of reduced instruction

set computing (RISC). The CH32V307 is a high-capacity, general-purpose microcontroller built on the RISC-V core, merging the adaptability of the RISC-V architecture with the comprehensive features of the microcontroller. It has 256KB flash memory and 64KB SRAM, providing powerful computing capabilities. It also has two built-in 12-bit DACs that can convert the digital chaotic signals calculated into analog voltage outputs. The design writes the chaotic map equation into the main loop to iterate continuously. The value of each iteration is linearly mapped to a digital range of 0-4095. It is written to the DAC registers to start conversion. The two DACs will convert the digital signals into analog voltage output to the channels of an oscilloscope, realizing the observation of chaotic graphs on the oscilloscope.

The whole process utilizes the CH32V307's computing power to continuously calculate the chaotic maps, and uses the built-in DACs to convert the digital chaotic signals into analog voltage form, finally displaying on the oscilloscope. This allows an in-depth study of chaotic systems. Fig. 16 shows the phase trajectories corresponding to each of the six chaotic maps. Fig. 17 demonstrates the offset boosting of the phase trajectories for chaotic maps MHM1 and MHM2 set at different parameters. The homogeneous multistability of chaotic maps MHM3 and MHM4 controlled by the initial values of $y(0)$ are shown in Fig. 18. Homogeneous multistability generated by the control of the initial values of $y(0)$ for the chaotic maps MHM5 and MHM6 are shown in Fig. 19.

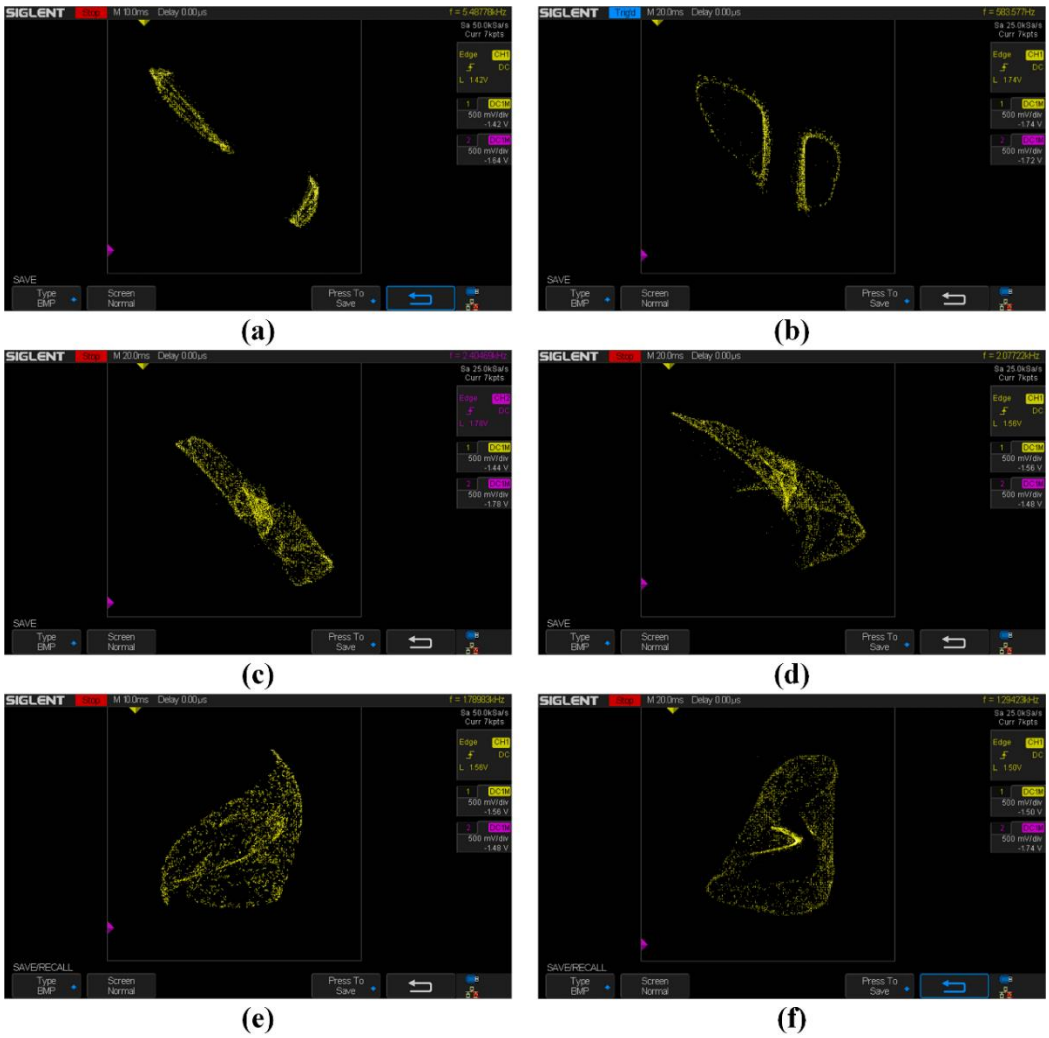

Fig. 16. Phase trajectories of six chaotic maps with different parameter settings: (a) MHM1, (b) MHM2, (c) MHM3, (d) MHM4, (e) MHM5, (f) MHM6.

Fig. 17. Phase trajectories with different settings of offset boosting values: (a) MHM1, (b) MHM2.

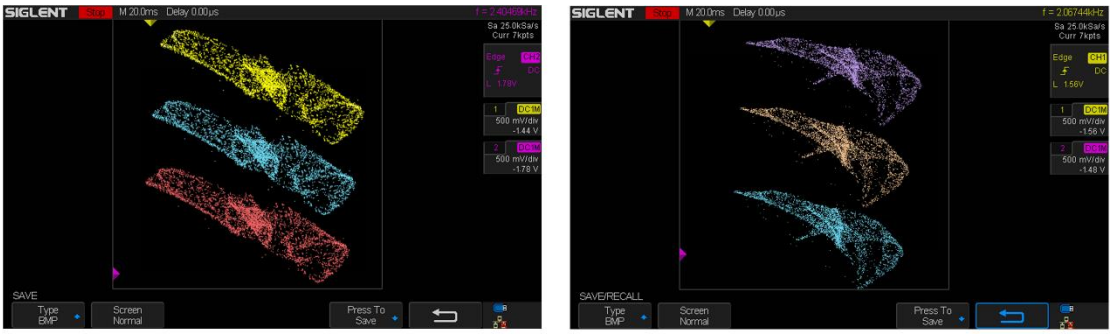

(a) **(b)**

Fig. 18. Discrete sequences in the chaotic maps MHM3 and MHM4 with different initial values of $y(0)$: (a) MHM3, (b) MHM4.

(a) **(b)**

Fig. 19. Discrete sequences in the chaotic maps MHM5 and MHM6 with different initial values of $y(0)$: (a) MHM5, (b) MHM6.

7. Conclusion

It has been found that many chaotic systems can be generated by introducing memristors in the Hénon map through various nonlinear functions. In these systems, when the system parameters are set appropriately, local offset boosting for single parameter control can be achieved thus providing more chaotic control options. This approach greatly enhances the range of controlled behaviors. The introduction of sine and cosine periodic functions further diversifies this control, enabling the initial conditions to govern offset boosting and facilitating the coexistence of homogeneous multistability within the phase space. When the system parameters are set differently, different numbers of attractors are generated. Moreover, by adjusting the excitation frequency of the memristors, the response state of the memristors can be adjusted and thus the control of chaos can be realized. These theoretical advancements have been practically verified through circuit implementations based on CH32 platform, confirming the potential value of this methodology for chaos regulation.

Acknowledgements

This work was supported by the Research and Innovation Training Projects of Dream Harvesting Space, and financially by the National Natural Science Foundation of China (Grant No.: 62371242).

Author Declarations

Conflict of Interest

The authors have no conflicts to disclose.

Author Contributions

Zhihao Wang: Formal analysis (equal); Methodology (equal); Software (equal); Visualization (equal); Writing – original draft. **Chunbiao Li:** Conceptualization (lead); Funding acquisition (equal); Methodology (equal); Writing – review & editing (equal). **Yongxin Li:** Methodology (equal); Software (equal); Circuit verification; Writing – review & editing (equal). **Irene Moroz:** Software (equal); Visualization (equal). **Haiyan Fu:** Software (equal); Visualization (equal).

Data Availability

The authors confirm that the data supporting the findings of this study are available within the article.

References

[1] Danca M-F, Kuznetsov N. Hidden chaotic sets in a Hopfield neural system. Chaos, Solitons & Fractals 2017;103:144–50.

[2] Hua Z, Zhou B, Zhou Y. Sine chaotification model for enhancing chaos and its hardware implementation. IEEE Transactions on Industrial Electronics 2018;66:1273–84.

[3] Jafari S, Sprott JC. Simple chaotic flows with a line equilibrium. Chaos, Solitons & Fractals 2013;57:79–84.

[4] Ma J. Energy function for some maps and nonlinear oscillators. Applied Mathematics and Computation 2024;463:128379.

[5] Bao H, Hu A, Liu W, Bao B. Hidden bursting firings and bifurcation mechanisms in memristive neuron model with threshold electromagnetic induction. IEEE Transactions on Neural Networks and Learning Systems 2019;31:502–11.

[6] Amigo JM, Kocarev L, Szczepanski J. Theory and practice of chaotic cryptography. Physics Letters A 2007;366:211–6.

[7] Hua Z, Zhu Z, Chen Y, Li Y. Color image encryption using orthogonal Latin squares and a new 2D chaotic system. Nonlinear Dynamics 2021;104:4505–22.

[8] Yuan F, Li Y, Wang G. A universal method of chaos cascade and its applications. Chaos: An Interdisciplinary Journal of Nonlinear Science 2021;31.

[9] Li C, Lei T, Liu Z. Offset parameter cancellation produces countless coexisting attractors. Chaos: An Interdisciplinary Journal of Nonlinear Science 2022;32.
[10] Bao H, Hua M, Ma J, Chen M, Bao B. Offset-control plane coexisting behaviors in two-memristor-based Hopfield neural network. IEEE Transactions on Industrial Electronics 2022;70:10526–35.
[11] Lai Q, Kuate PDK, Liu F, Iu HH-C. An extremely simple chaotic system with infinitely many coexisting attractors. IEEE Transactions on Circuits and Systems II: Express Briefs 2019;67:1129–33.
[12] Chen C, Min F, Cai J, Bao H. Memristor Synapse-Driven Simplified Hopfield Neural Network: Hidden Dynamics, Attractor Control, and Circuit Implementation. IEEE Transactions on Circuits and Systems I: Regular Papers 2024.
[13] Zhang S, Li C, Zheng J, Wang X, Zeng Z, Chen G. Memristive Autapse-Coupled Neuron Model With External Electromagnetic Radiation Effects. IEEE Transactions on Industrial Electronics 2022.
[14] Peng Y, Sun K, He S. A discrete memristor model and its application in Hénon map. Chaos, Solitons & Fractals 2020;137:109873.
[15] Li C, Sprott JC. Variable-boostable chaotic flows. Optik 2016;127:10389–98.
[16] Li C, Yi C, Li Y, Mitro S, Wang Z. Offset boosting in a discrete system. Chaos: An Interdisciplinary Journal of Nonlinear Science 2024;34.
[17] Zhang S, Wang X, Zeng Z. A simple no-equilibrium chaotic system with only one signum function for generating multidirectional variable hidden attractors and its hardware implementation. Chaos: An Interdisciplinary Journal of Nonlinear Science 2020;30.
[18] Yu F, Qian S, Chen X, Huang Y, Cai S, Jin J, et al. Chaos-based engineering applications with a 6D memristive multistable hyperchaotic system and a 2D SF-SIMM hyperchaotic map. Complexity 2021;2021:1–21.
[19] Li Y, Li C, Zhang S, Chen G, Zeng Z. A self-reproduction hyperchaotic map with compound lattice dynamics. IEEE Transactions on Industrial Electronics 2022;69:10564–72.
[20] Zhang Y, Hua Z, Bao H, Huang H, Zhou Y. An $ n $-dimensional chaotic system generation method using parametric pascal matrix. IEEE Transactions on Industrial Informatics 2022;18:8434–44.
[21] Wu C, Sun K. Generation of multicavity maps with different behaviours and its DSP implementation. Chaos, Solitons & Fractals 2022;159:112129.
[22] Pham V-T, Volos C, Jafari S, Kapitaniak T. Coexistence of hidden chaotic attractors in a novel no-equilibrium system. Nonlinear Dynamics 2017;87:2001–10.
[23] Ma J, Wu F, Ren G, Tang J. A class of initials-dependent dynamical systems. Applied Mathematics and Computation 2017;298:65–76.
[24] Zhang S, Li C, Zheng J, Wang X, Zeng Z, Peng X. Generating any number of initial offset-boosted coexisting Chua's double-scroll attractors via piecewise-nonlinear memristor. IEEE Transactions on Industrial Electronics 2021;69:7202–12.

[25] Lin H, Wang C, Cui L, Sun Y, Xu C, Yu F. Brain-like initial-boosted hyperchaos and application in biomedical image encryption. IEEE Transactions on Industrial Informatics 2022;18:8839–50.
[26] Zhang L-P, Liu Y, Wei Z-C, Jiang H-B, Lyu W-P, Bi Q-S. Extremely hidden multi-stability in a class of two-dimensional maps with a cosine memristor. Chinese Physics B 2022;31:100503.
[27] Yuan F, Yu X, Deng Y, Li Y, Chen G. A Cu-Doped TiO 2-x Nanoscale Memristor With Application to Heterogeneous Coupled Neurons. IEEE Transactions on Industrial Electronics 2023.
[28] Bao B, Ma Z, Xu J, Liu Z, Xu Q. A simple memristor chaotic circuit with complex dynamics. International Journal of Bifurcation and Chaos 2011;21:2629–45.
[29] Yuan F, Jin Y, Li Y. Self-reproducing chaos and bursting oscillation analysis in a meminductor-based conservative system. Chaos: An Interdisciplinary Journal of Nonlinear Science 2020;30.
[30] Chua L. Memristor-the missing circuit element. IEEE Transactions on Circuit Theory 1971;18:507–19.
[31] Chen C, Min F, Cai J, Bao H. Memristor Synapse-Driven Simplified Hopfield Neural Network: Hidden Dynamics, Attractor Control, and Circuit Implementation. IEEE Transactions on Circuits and Systems I: Regular Papers 2024.
[32] Liu J, Liu S, Sprott JC. Adaptive complex modified hybrid function projective synchronization of different dimensional complex chaos with uncertain complex parameters. Nonlinear Dynamics 2016;83:1109–21.
[33] Zhang S, Zheng J, Wang X, Zeng Z, He S. Initial offset boosting coexisting attractors in memristive multi-double-scroll Hopfield neural network. Nonlinear Dynamics 2020;102:2821–41.
[34] Zhang L-P, Liu Y, Wei Z-C, Jiang H-B, Bi Q-S. A novel class of two-dimensional chaotic maps with infinitely many coexisting attractors. Chinese Physics B 2020;29:060501.
[35] Sprott JC, Wang X, Chen G. Coexistence of point, periodic and strange attractors. International Journal of Bifurcation and Chaos 2013;23:1350093.